2007 IEEE International Conference on
Robotics and Automation
Roma, Italy, 10-14 April 2007

Accurate Force Control and Motion Disturbance Rejection for Shape Memory Alloy Actuators

Yee Harn Teh and Roy Featherstone

Abstract— **This paper presents simulation and experimental results for closed-loop force control of single-wire Shape Memory Alloy (SMA) actuators. The simulation uses a model derived from the frequency response analysis of SMA. Although the large-scale response has hysteresis and nonlinearities, small-signal frequency response analysis is possible on SMA wires, with detectable force response at frequencies up to 100 Hz. The model has been demonstrated to accurately predict closed-loop behaviour. A high performance force control system using PID control is also demonstrated. Results show fast convergence, and excellent setpoint and tracking accuracy with practically no sign of limit cycles. Experimental results in this paper are the first to have demonstrated stable and accurate response with good rejection of large motion disturbances.**

I. Introduction

Actuators based on Shape Memory Alloys have a variety of advantages that make them suitable for niche applications in robotics. They include: high force-to-weight ratio, mechanical simplicity, compactness, easy miniaturization, and clean, silent operation. Their main disadvantage is very low energy efficiency (e.g. around 1 %). However, two other disadvantages — slow speed and inaccuracy — can be solved by better actuator and control system design.

Early work on fast, accurate motion control was performed by Grant [1], who used a two-stage relay controller and an antagonistic pair of SMA actuators. However, his control system showed large limit cycles, which have been subsequently improved upon by [2], [3]. Grant was also the first to demonstrate fast constrained force control with SMA actuators [4]. Other works on force control of SMA include [5], [6].

In this paper, we will present a new pole-zero model obtained from small-signal frequency response analysis of SMA wire actuators which accurately predicts closed-loop performance. This paper is the first to show that small-signal frequency response analysis is possible in spite of the hysteresis and nonlinearity in SMA. The results show that the phase is independent of stress and strain, and the magnitude varies by only a small amount.

Using the model in simulation, a set of PID control parameters is obtained. The PID controller is then implemented and fine-tuned online to obtain better results. The experimental results show very high setpoint and tracking accuracy with no sign of limit cycles, which are also in agreement with the simulation. This paper is also the first to present experimental results for force control of SMA actuators in the presence of motion disturbances. The results demonstrate good rejection of motion disturbances.

The results in this paper form a crucial step in our research to achieve fast, accurate force and motion control of antagonistic pairs of SMA actuators.

Both Y. H. Teh and R. Featherstone are with Department of Information Engineering, Research School of Information Sciences and Engineering, The Australian National University, Canberra, ACT 0200, Australia yee.teh|roy.featherstone@rsise.anu.edu.au

II. Experimental Test Bed

Both the frequency response analysis and the force control experiments were conducted using the test bed shown in Figure 1. The test bed can accommodate two SMA wires arranged antagonistically about a rotating pulley and shaft housing. The SMA wires used in these experiments are 100μm-diameter Flexinol[1] with an Austenite finish temperature of 90°C. These are commercially produced NiTi alloy wires capable of contracting millions of times, with a normal working strain of 4 %. The wires in our test bed are 80 cm long.

Other major components of the test rig are: (1) two sensitive load cells capable of accurate, high-bandwidth force measurements in the $\pm$ 9 N range with a resolution of 0.3 mN, (2) a servo-controlled precision linear slide capable of applying precise strain profiles or motion disturbances to the SMA wires, (3) precision DC current amplifiers for driving the SMA wires, and (4) a DS1104 real-time control board from dSPACE upon which any desired SMA control system can be implemented.

The two load cells, one for each SMA wire, are housed at the bottom of the test rig together with the strain gauge amplifiers and electronic force overload monitor circuits as shown in Figure 1(c). Visible in this figure, each SMA wire is doubled-up, so that both ends are electrically connected to a tiny PCB attached at the end of each load cell. Note that only one SMA wire is installed for the experiments reported in this paper.

The linear slide is positioned at the top of the test rig as shown in Figure 1(b). The slide also houses the rotating pulley and shaft with a locking mechanism and an optical shaft encoder. The pulley is intended for use with antagonistic pairs of SMA wires. For the experiments described in this paper, the pulley is locked mechanically.

III. Modelling

In control system design, a plant model is invaluable as a design aid. However, developing a mathematical model that captures the behavior of a Shape Memory Alloy as it undergoes temperature, stress and phase changes is a complicated

[1]Flexinol is a trademark of Dynalloy, Inc. (http://www.dynalloy.com)

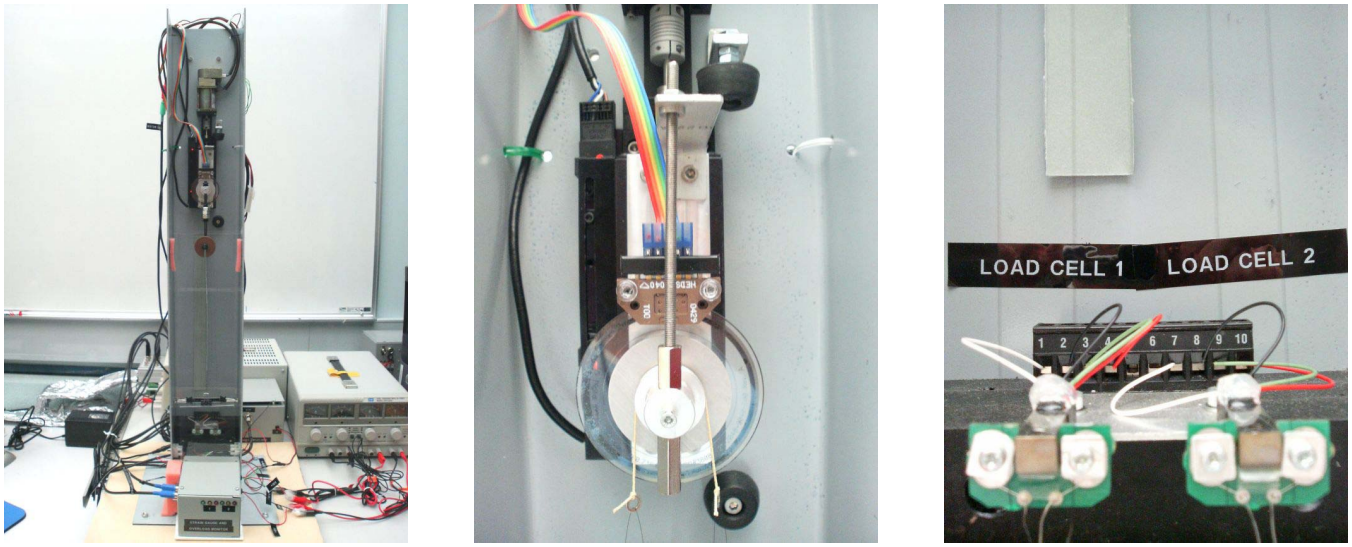

(a) (b) (c)

Fig. 1. The experimental test bed (a), detailed views of the linear slide (b) and load cell housings (c).

and challenging problem. Some of these models can be found in [1], [7], [8], [9], [10]. Using frequency response analysis, we propose a model based on the input-output relationship of the SMA over the frequency range of 0.1 – 100 Hz. We are interested in studying the response at frequencies of up to 100 Hz because we have observed limit cycles at frequencies of 20 – 30 Hz in our past experiments. To understand how to quench these limit cycles, it is important to investigate the high frequency dynamics of SMA.

The frequency response of a linear system describes how the system responds to sinusoidal inputs. The large-scale response of SMA is nonlinear and is dominated by the presence of a wide hysteresis loop in the phase transformation. However, under small-signal conditions, the hysteresis loop is reduced and the material behaves almost linearly. This behaviour allows us to perform small-signal frequency response analysis and obtain a linear transfer function model of the SMA. A practical advantage of modelling using this method is the repeatability of the results.

Firstly, a biased, positive sinusoidal power signal is generated, and a corresponding current signal is calculated based on a nominal SMA electrical resistance value. That current signal is sent to the DC current amplifier to drive an SMA wire. Once steady-state is achieved, the corresponding force output of the SMA actuator is recorded over a suitable period. The above procedure is repeated for suitable spot frequencies over the 0.1 – 100 Hz range.

Note that the mean (DC) value of the input power signal is kept constant over the frequency range so that the mean force output is fairly constant, although the magnitude of the AC input signal is varied. At the lowest frequency, the magnitude of the sinusoid is kept small, so that only small temperature variations result; but the magnitude is increased at higher frequencies so that there is still a detectable force signal. Strictly speaking, it is the temperature fluctuation that is the small signal, not the heating power. The SMA wire is also shielded within the test bed to reduce the effects of air ventilation on wire temperature.

The recorded data are then used to estimate the force amplitudes and phase shifts of the actuator over the frequency range using a least-squares algorithm. The algorithm is sufficiently robust to reject the noise and harmonic distortion present in the force signal, and the estimates have been averaged over many cycles. A measure of the dynamic response of the system can now be built and plotted using Bode diagrams. The above procedures are repeated using different mean values of the input power signal and varying linear slide positions to span the full range of allowable stresses and strains in the SMA.

The solid black curves in Figure 2 show the experimental Bode plots of the system under varying stress and strain conditions. Each curve represents one stress-strain combination. The magnitude in decibels (dB) is given by:

$$Magnitude = 20 \log \frac{ForceAmplitude}{MeanACPower}. \quad (1)$$

It can be seen that the magnitude plots vary by a small amount under different conditions. The phase plots however, are invariant to stress and strain. This characteristic is useful in determining the approximate pole-zero model for the system.

Based on the Bode plots, a model of the plant can be extracted to satisfy the following relationship between input power and force for a single SMA wire:

$$F(s) = G(s)P(s), \quad (2)$$

where $F(s)$ is the force output response, $P(s)$ is the input power signal, and $G(s)$ is the transfer function.

Equation 2 describes an explicit input-output relationship for the heating and cooling of a single SMA wire which

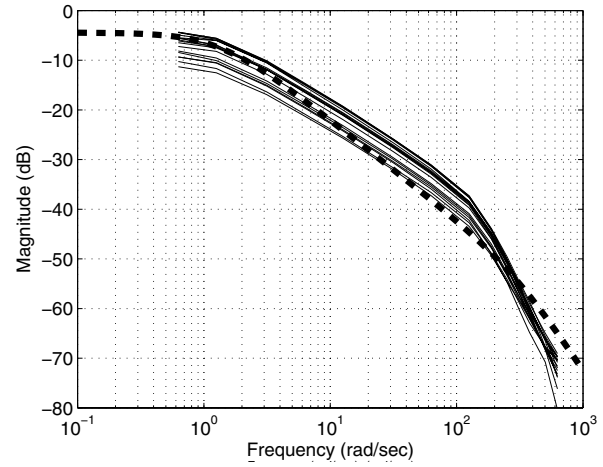

(a)

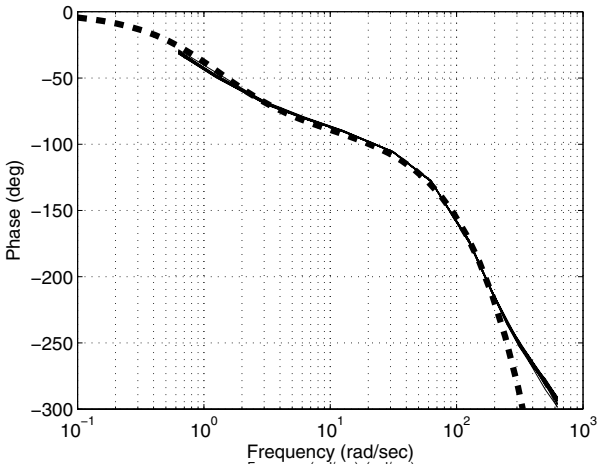

(b)

Fig. 2. Bode magnitude and phase plots of the frequency response data and the derived transfer function model, $G(s)$. Solid black lines = frequency response experimental data. Dashed black line = model.

is the crucial key in determining the force model for the SMA actuator. To model the data in Figure 2, we chose a transfer function consisting of a 2^{nd} order linear system and a transport delay. The analytical expression for this transfer function is

$$G(s) = \frac{Ke^{-sL}}{(T_1 s + 1)(T_2 s + 1)}, \tag{3}$$

and a suitable value that fits the experimental data is

$$G(s) = \frac{0.6e^{-0.0085s}}{(0.7579s + 1)(0.003183s + 1)}. \tag{4}$$

The Bode magnitude and phase plots for this model are shown as the dashed black curves in Figure 2. The model can be observed to accurately match the experimental Bode plots up to a frequency of 200 rad/sec.

IV. Force Control

A. Controller Design

We investigated the force control of a single-wire SMA actuator using a proportional-integral-derivative (PID) controller. The controller transfer function is given by

$$D(s) = K_P(1 + \frac{1}{T_I s} + T_D s), \tag{5}$$

where K_P, T_I and T_D are the proportional, integral and derivative gains respectively. Using the model in simulation, the feasibility of using PID control in SMA force control is tested and a set of control parameters obtained. The PID controller is then implemented and fine-tuned online to obtain better results. The final parameter values are K_P = 50, T_I = 0.025 and T_D = 0.02. Because the actual SMA wire can be damaged by overheating, a power limit of 5 W is applied to the control system in both simulation and the experiment. To illustrate the accuracy of the small-signal model, it was found that the model predicts limit cycles as K_P is increased to 82; and the value at which limit cycles occur in practice is when K_P = 90. All simulations are conducted using $Simulink^{TM}$. Experiments are conducted using the test bed of Figure 1.

B. Step Response

Both the simulated and experimental responses to a series of force step inputs from 1 N to 3 N are shown in Figure 3.

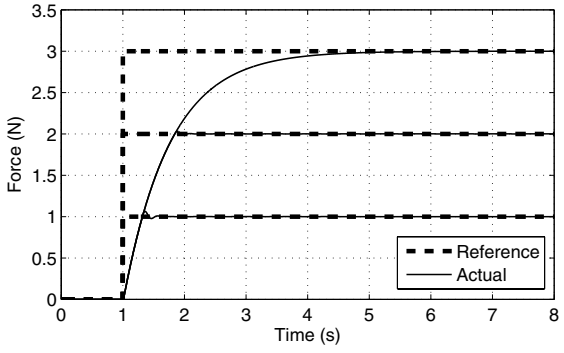

(a)

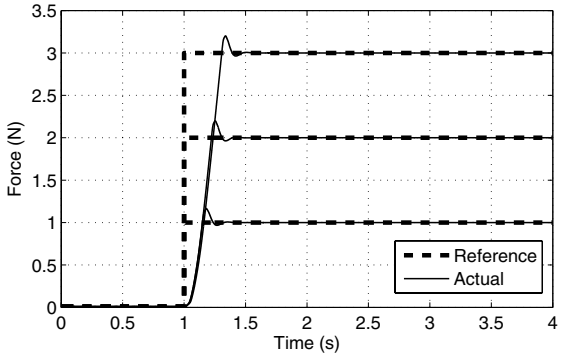

(b)

Fig. 3. (a) Simulated and (b) experimental closed loop force step response for a single SMA actuator at steps of 1, 2 and 3 N.

It should be noted that 3 N is the maximum rated pulling force for a doubled-up 100μm-diameter Flexinol wire. The same PID controller parameters are used in both simulation and experiment.

It is clear from these graphs that the small-signal model is a poor predictor of the large-signal response of the SMA wire. In particular, it underestimates the large-signal gain. It can be seen that the simulation has reached saturation with the power limit of 5 W. If the power limit is increased, then the simulation will agree better with the experiments.

In Figure 3(b), it can be seen that the rise times are approximately 0.2 s, 0.3 s and 0.4 s respectively for step inputs of 1 N, 2 N and 3 N. Maximum overshoot is approximately 10 %. The simulated and experimental force tracking errors are not shown; but these errors are measured to be less than 0.001 N at steady state, and no limit cycle is observed.

For the experimental responses, an initial desired force input of 0.01 N has been applied before time = 1 s so that the actuator will not start out slack in the test bed. Since the actuator is already warm, this taut configuration allows it to contract faster.

C. Tracking Response

Using the same controller parameters, the simulated and experimental closed loop tracking responses are examined. The responses to sinusoidal force commands at frequencies of 1 Hz and 2 Hz, as well as DC offsets of 1 N and 2 N have been investigated.

Figures 4(a) and 4(b) show the force tracking errors in response to force commands of the form $c+0.2\sin(2\pi ft)$ N, with $c \in \{1, 2\}$ and f = 1 Hz. Both simulated and experimental results are presented. Despite the different DC offsets, the curves in Figures 4(a) and 4(b) are similar. The model predicts a peak tracking error of about 0.005 N, and the experimental results show a tracking error slightly less than 0.002 N, but the two curves are approximately in phase. The model is therefore overestimating the magnitude of the tracking error by a factor of 3, but is getting the phase right. A tracking error of 0.002 N is 0.067 % of the 3 N force output range of the actuator.

Figures 4(c) and 4(d) show the tracking errors in response to force commands of the form $c + 0.1\sin(2\pi ft)$ N, with $c \in \{1, 2\}$ and f = 2 Hz. Once again, the curves in Figures 4(c) and 4(d) are very similar, indicating that the DC offset makes little difference. The model predicts a peak tracking error of about 0.012 N, and the experimental results show a tracking error of about 0.003 N, but the two curves are approximately in phase. The model is therefore overestimating the magnitude of the tracking error by about a factor of 4, but is getting the phase right. A tracking error of 0.003 N is 0.1 % of the output range of the actuator.

If the magnitude of the AC component of the command signal is increased, then there comes a point where the simulation goes into saturation (by hitting the power limits). When this occurs, the simulator no longer makes useful predictions.

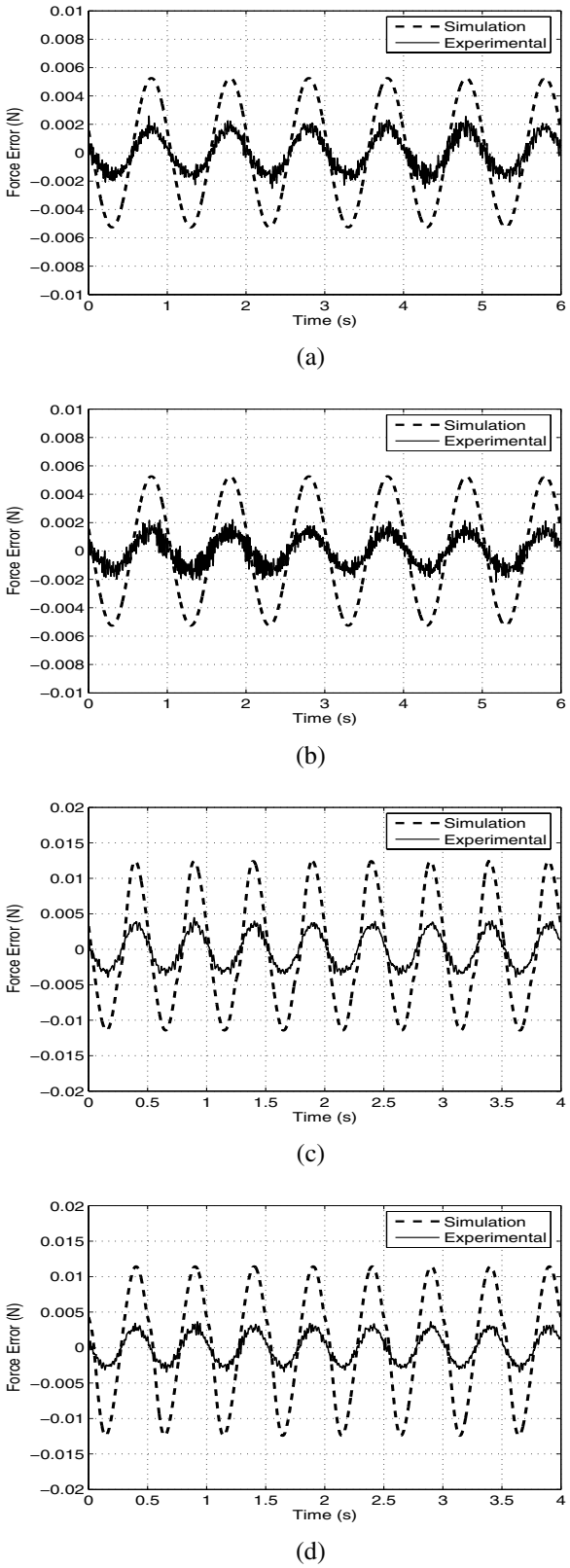

Fig. 4. (a) Force tracking errors to $1 + 0.2\sin(2\pi ft)$ N force command with f = 1 Hz, (b) force tracking errors to $2 + 0.2\sin(2\pi ft)$ N force command with f = 1 Hz, (c) force tracking errors to $1 + 0.1\sin(2\pi ft)$ N force command with f = 2 Hz, and (d) force tracking errors to $2 + 0.1\sin(2\pi ft)$ N force command with f = 2 Hz.

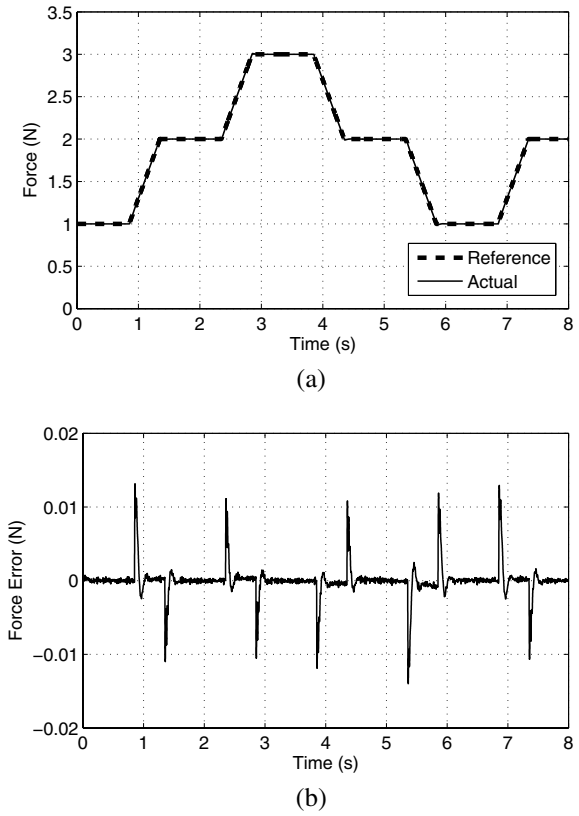

Fig. 5. (a) Experimental closed loop force tracking response, and (b) force errors, for a single SMA actuator using a series of ramp and constant inputs.

The experimental response to a series of constant and ramp signals has also been recorded as shown in Figure 5. The ramps have slopes of $\pm\,2\,\mathrm{N.s}^{-1}$. The sudden changes in slope produce the narrow error spikes in Figure 5(b). It is also observed, however, that the control system can rapidly correct the errors. Accuracy at steady state is again better than 0.001 N.

V. Presence of Motion Disturbances

To investigate how the control system performs under the influence of motion disturbances, the SMA actuator is subjected to strain changes by vertically servoing the linear slide to follow a 4 mm magnitude sinusoidal signal of 0.33 Hz. The 4 mm disturbance constitutes 25 % of the SMA strain range under normal conditions. Since the 80 cm long SMA wire is doubled up, its effective strain range is 1.6 cm.

Force tracking performance of a $1+0.2\sin(2\pi ft)$ N signal at f = 1 Hz, under strain disturbance throughout the experiment, is presented in Figure 6. The strain disturbance clearly degrades the response compared to Figure 4(a). The force tracking error in Figure 6(b) contains a 0.33 Hz error signal due to the disturbance, which is superimposed on the smaller 1.0 Hz error, and high-frequency error spikes. The force error spikes are caused by position error spikes in the linear slide motion control system, shown in Figure 6(c). These spikes have been observed to occur at every 30° rotation of the

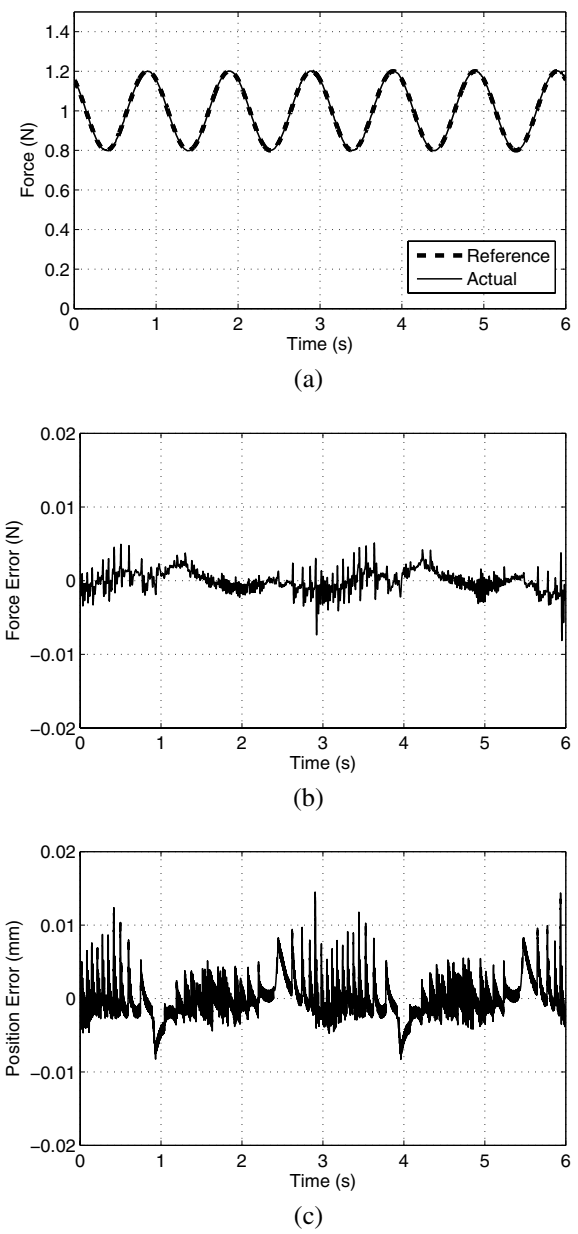

Fig. 6. Experimental closed loop force tracking response for a single SMA actuator, under a 4 mm magnitude sinusoidal motion disturbance of 0.33 Hz, using reference force signal of $1+0.2\sin(2\pi ft)$ N. (a) Force tracking at f = 1.0 Hz, (b) Force error from (a), and (c) Linear slide position error.

servo motor, and are caused by a hardware fault in the linear slide. The force controller cannot completely eliminate the effects of the sharp position spikes due to their high-frequency components.

Although the performance of the closed loop response has been affected, its accuracy is fairly good. The response is stable and is able to reject the 0.33 Hz motion disturbances throughout the experiment. The force tracking error of Figure 6(b) has a maximum amplitude of 0.005 N or less, except for a few of the biggest spikes.

VI. Applications and Current Work

The experiments and results completed in this paper are part of a larger research in which we aim to achieve fast and accurate force and motion control of antagonistic SMA actuator pairs. The use of the small-signal model as a control design aid has been shown, and the force control of a single-wire SMA actuator has been demonstrated.

The research forms the enabling basis for our current work on the differential force control as well as the combined force and motion control of an antagonistic SMA actuator pair. The usefulness of the model in simulation will be more apparent when the design of high-performance controllers becomes more complicated, due to the requirement to control two SMA wires rather than only one, and due to our planned incorporation of the rapid heating algorithm described in [11].

Previous research in feedback control of SMA under the influence of heavy external loadings has usually resulted in large limit cycles. A high-bandwidth, small-signal force control system may be able to eliminate these limit cycles, thereby allowing much better position accuracy to be obtained. This has potential commercial applications such as in camera anti-shake mechanisms [12] or vibration control [13]. SMA actuators can also be used in micro-actuator applications [14] such as micro-grippers, valves or linear actuators. Electric motors may not be suitable in these miniaturised applications due to cost, weight and space problems, and other actuator technologies such as piezo-actuators cannot generate sufficiently large motions.

VII. Conclusion

In this paper, we have successfully demonstrated the small-signal frequency response analysis of SMA actuator wires. The fact that a pole-zero model can be extracted from this analysis is worth mentioning as no such attempt has been made in the literature. The model is then used to aid the design of a PID controller and also used to simulate SMA closed loop response.

Our results show that this model accurately predicts the stability and small-signal tracking accuracy of the SMA wire's closed-loop response under PID control; but it underestimates the large-signal heating and cooling rates of the wire.

Using this PID controller, force control experiments have been carried out on actual SMA wires. Experimental results show excellent setpoint and tracking accuracy with no limit cycles. Reasonably fast response has also been demonstrated with good tracking of a 2.0 Hz force command. The experimental error amplitudes are observed to be 0.003 N, which is only 0.1 % of the 3 N maximum force range of the SMA wire. Finally, this paper presents results that demonstrate, for the first time, accurate tracking of force commands in the presence of large motion disturbances, with an error amplitude of only 0.005 N.

References

[1] D. Grant, *Accurate and Rapid Control of Shape Memory Alloy Actuators*, PhD Thesis TR-CIM-99-11, Centre for Intelligent Machines, McGill University, 1999.

[2] M.H. Elahinia, T. M. Seigler, D. J. Leo and M. Ahmadian, "Nonlinear Stress-Based Control of a Rotary SMA-Actuated Manipulator", *Journal of Intelligent Material Systems and Structures*, vol. 15, no. 6, 2004, pp. 495-508.

[3] Y. H. Teh and R. Featherstone, "Experiments on the Performance of a 2-DOF Pantograph Robot Actuated by SMA Wires", *in Proceedings of the Australasian Conference on Robotics and Automation*, Canberra, December 2004.

[4] D. Grant and V. Hayward, "Constrained Force Control of Shape Memory Alloy Actuators", *in Proceedings of the IEEE International Conference on Robotics and Automation*, San Francisco, CA, April 2000.

[5] S. B. Choi, Y. M. Han, J. H. Kim and C. C. Cheong, "Force Tracking Control of a Flexible Gripper Featuring Shape Memory Alloy Actuators", *Mechatronics*, vol. 11, 2001, pp. 677-690.

[6] T. Hino and T. Maeno, "Development of a Miniature Robot Finger with a Variable Stiffness Mechanism Using Shape Memory Alloy", *in Proceedings of the International Simposium on Robotics and Automation*, Querétaro, Mexico, 2004.

[7] S. Majima, K. Kodama and T. Hasegawa, "Modeling of Shape Memory Alloy Actuator and Tracking Control System with the Model", *IEEE Transactions on Control System Technology*, vol. 9, no. 1, 2001, pp. 54-59.

[8] Y. Matsuzaki and H. Naito, "Macroscopic and Microscopic Constitutive Models of Shape Memory Alloys Based on Phase Interaction Energy Function: a Review", *Journal of Intelligent Material Systems and Structures*, vol. 15, 2004, pp. 141-155.

[9] S. M. Dutta and F. H. Ghorbel, "Differential Hysteresis Modeling of a Shape Memory Alloy Wire Actuator", *IEEE/ASME Transactions on Mechatronics*, vol. 10, no. 2, 2005, pp. 189-197.

[10] R. B. Gorbet, D. W. L. Wang and K. A. Morris, "Preisach Model Identification of a Two-Wire SMA Actuator", *in Proceedings of the IEEE International Conference on Robotics and Automation*, 1998.

[11] R. Featherstone and Y. H. Teh, "Improving the Speed of Shape Memory Alloy Actuators by Faster Electrical Heating", *in Proceedings of the International Symposium on Experimental Robotics*, Singapore, June 2004.

[12] O. Masamichi, "Drive Apparatus, Drive System, and Drive Method", *US Patent Number 2006150627*, Konica Minolta Holdings Inc., 13 July 2006.

[13] C. Liang and C. A. Rogers, "Design of Shape Memory Alloy Springs with Applications in Vibration Control", *Journal of Vibration and Acoustics*, vol. 115, January 1993, pp. 129-135.

[14] M. Kohl, *Shape Memory Microactuators*, Springer, 2004.